Brain Topography (2019) 32:178–191
https://doi.org/10.1007/s10548-018-0680-5

ORIGINAL PAPER

Ictal Source Locations and Cortico–Thalamic Connectivity in Childhood Absence Epilepsy: Associations with Treatment Response

Ailiang Miao[1] · Yingxin Wang[1] · Jing Xiang[2] · Qianqian Liu[3] · Qiqi Chen[4] · Wenchao Qiu[5] · Hongxing Liu[1] · Lu Tang[1] · Yuan Gao[1] · Caiyun Wu[1] · Yuanwen Yu[1] · Jintao Sun[1] · Wenwen Jiang[1] · Qi Shi[1] · Tingting Zhang[1] · Zheng Hu[6] · Xiaoshan Wang[1]

Received: 6 April 2018 / Accepted: 1 October 2018 / Published online: 5 October 2018

Abstract

Childhood absence epilepsy (CAE), the most common pediatric epilepsy syndrome, is usually treated with valproic acid (VPA) and lamotrigine (LTG) in China. This study aimed to investigate the ictal source locations and functional connectivity (FC) networks between the cortices and thalamus that are related to treatment response. Magnetoencephalography (MEG) data from 25 patients with CAE were recorded at 300 Hz and analyzed in 1–30 Hz frequency bands. Neuromagnetic sources were volumetrically scanned with accumulated source imaging. The FC networks between the cortices and thalamus were evaluated at the source level through a connectivity analysis. Treatment outcome was assessed after 36–66 months following MEG recording. The children with CAE were divided into LTG responder, LTG non-responder, VPA responder and VPA non-responder groups. The ictal source locations and cortico–thalamic FC networks were compared to the treatment response. The ictal source locations in the post-dorsal medial frontal cortex (post-DMFC, including the medial primary motor cortex and the supplementary sensorimotor area) were observed in all LTG non-responders but in all LTG responders. At 1–7 Hz, patients with fronto–thalamo–parietal/occipital (F–T–P/O) networks were older than those with fronto–thalamic (F–T) networks or other cortico–thalamic networks ($p = 0.000$). The duration of seizures in patients with F–T–P/O networks at 1–7 Hz was longer than that in patients with F–T networks or other cortico–thalamic networks ($p = 0.001$). The ictal post-DMFC source localizations suggest that children with CAE might experience initial LTG monotherapy failure. Moreover, the cortico–thalamo–cortical network is associated with age. Finally, the cortico–thalamo–cortical network consists of anterior and posterior cortices and might contribute to the maintenance of discharges.

Keywords Childhood absence epilepsy · Magnetoencephalography · Source location · Cortico–thalamic network · Treatment response

Introduction

Childhood absence epilepsy (CAE), as the most common form of pediatric epilepsy, accounts for 10–17% of all cases of childhood-onset epilepsy (Berg et al. 2000; Jallon et al.

Handling Editor: Stefano Seri.

Ailiang Miao and Yingxin Wang have contributed equally to this work.

✉ Xiaoshan Wang
xiaoshanwang1971@163.com

[1] Department of Neurology, Nanjing Brain Hospital, Nanjing Medical University, Guang Zhou Road 264, Nanjing 210029, Jiangsu, China

[2] MEG Center, Division of Neurology, Cincinnati Children's Hospital Medical Center, Cincinnati, OH 45220, USA

[3] Department of Pediatrics, Nanjing Jiangning Hospital, Nanjing 210029, Jiangsu, China

[4] MEG Center, Nanjing Brain Hospital, Nanjing 210029, Jiangsu, China

[5] Department of Neurology, The Affiliated Huaian Hospital of Xuzhou Medical University, Huai'an, China

[6] Department of Neurology, Nanjing Children's Hospital, Nanjing 210029, Jiangsu, China

2001). The syndrome is characterized by brief (approximately 5–30 s) disruptions in consciousness, typically beginning at 4–8 years of age (International League Against Epilepsy 1989). The classic electroencephalogram (EEG) shows generalized 3 Hz spike-wave discharges (SWDs) with normal background activity (International League Against Epilepsy 1989; Loiseau et al. 1995). Often misperceived as a benign form of epilepsy, CAE is associated with long-term psychosocial difficulties and cognitive deficits in patients (Bouma et al. 1996; Pavone et al. 2001; Wirrell et al. 1997). Ethosuximide (ETX), valproic acid (VPA), and lamotrigine (LTG) are commonly used to treat CAE (Wheless et al. 2005). The freedom from treatment failure (FFF) rates of initial monotherapy at 16–20 weeks and at 12 months are 45% and 53% for ETX, 44% and 58% for valproate (VPA), and 21% and 29% for LTG, respectively (Glauser et al. 2010, 2013). Unfortunately, information about ETX treatment is not available in China. Moreover, the reason for the different efficacy rates of the three drugs remains poorly understood. The frontal cortex, parietal cortex, occipital lobe and thalamus are crucial regions in the initiation and propagation of absence seizure according to previous scalp EEG, EEG–fMRI and magnetoencephalography (MEG) studies (Amor et al. 2009; Bai et al. 2010; Carney et al. 2010; Gupta et al. 2011; Masterton et al. 2013; Meeren et al. 2002; Miao et al. 2014a, b; Moeller et al. 2008; Szaflarski et al. 2010; Vaudano et al. 2009; Tang et al. 2015; Tenney et al. 2013, 2014; Westmijse et al. 2009). Furthermore, the source locations of ictal SWDs vary among reports. SWDs occur through repetitive cyclic activity between the cortex and thalamus (Bai et al. 2010; Miao et al. 2014a; Szaflarski et al. 2010; Tang et al. 2015; Tenney et al. 2013, 2014). The thalamus is a relevant resonator for the maintenance of SWD (Meeren et al. 2002, 2005; van Luijtelaar and Sitnikova 2006). However, the source locations and network characteristics reported are not used to guide clinical treatment. Research is needed on whether the ictal source location may explain the FFF rates of VPA and LTG and on whether it may serve as an imaging marker to aid in the determination of appropriate. The duration discharges vary in absence seizures (Gadad et al. 2018). The contributions of the ictal fronto–thalamo–parietal/occipital (F–T–O/P) network and the fronto–thalamic (F–T) network to duration discharges are yet to be determined. Furthermore, research is needed to determine if the cortico–thalamic network is associated with age.

In the present study, we performed a group analysis of the ictal MEG data from 25 patients with CAE at 1–30 Hz in CAE. The source locations and cortico–thalamic networks were analyzed between AED responders and AED non-responders to search for imaging markers contributing to the efficacy of AEDs. AED responders indicate children with CAE who benefit from their initial monotherapy. In contrast, children who do not improve with initial monotherapy were called AED non-responders.

Methods

Subjects

Twenty-five children with CAE aged 4–11 years old were, diagnosed and recruited from Nanjing Brain Hospital and the Neurology Division at Nanjing Children's Hospital from September 2012 to February 2015. A total of 25 patients with CAE, who were screened and met the inclusion criteria, were included in this study. At 36–66 months after MEG recording, we performed follow-up assessments of all patients and gathered information about AEDs and prognosis. The clinical details of the patients are shown in Table 1. Similar to our previous research (Miao et al. 2014a, b), the inclusion criteria were as follows: (1) a diagnosis of typical CAE without automatisms, eye rolling or blinking and that was consistent with the International League Against Epilepsy Proposal for Revised Classification of Epilepsies and Epileptic Syndromes; (2) normal brain magnetic resonance imaging (MRI); bilaterally synchronous 3–4 Hz SWDs on a normal background with at least one electroclinical seizure lasting 10 s or more; and less than 5-mm head movement during MEG recordings; and (3) normal development; normal neurological examination. The exclusion criteria were as follows: (1) history of other major neurologic or psychiatric diseases; (2) presence of clinically significant systemic disease; (3) presence of metal implants, such as cochlear devices and pacemakers that would strongly interfere with MEG data; and (4) inability to keep head still during MRI scans and/or MEG recordings. The medical ethics committees of Nanjing Children's Hospital, Nanjing Brain Hospital, and Nanjing Medical University approved the present study. All participants and their guardians signed written informed consent forms.

MEG Recording

All subjects were instructed to stay up late at night and wake up early in the morning before MEG recordings to reduce sleeping time to increase the chance of absence seizures during MEG recordings. The MEG data were recorded using a whole-head CTF 275-Channel MEG system (VSM Medical Technology Company, Canada) in a magnetically shielded room (MSR). Before MEG recording, three small coils were attached to the nasion and to the left and right preauricular points of each subject. The subjects' head positions relative to the MEG sensors were measured using the three coils. The system allowed head localization with an accuracy of 1 mm and head movement

Table 1 Clinical patient's data

Patients	Sex (F/M)	Onset age	Seizure frequency (time/day)	Seizures duration (> 10 s)	AEDs before MEG recording	Initial AEDs	AEDs added	Revisit time after MEG recording (months)	Seizure controlled (Y/N)
1	F	9	5	1	No	VPA	No	55	Y (AEDs stopped)
2	F	10	8	2	No	LTG	VPA	39	Y
3	F	9	5	1	No	LTG	No	57	Y
4	M	8	8	2	No	VPA	No	58	Y
5	F	7	20	1	No	Lost	Lost	Lost	Lost
6	F	8	20	2	No	LTG	No	36	Y (AEDs stopped)
7	M	8	10	1	No	VPA	No	59	Y
8	F	9	6	1	No	LTG	VPA	54	Y
9	M	10	10	1	No	Lost	Lost	Lost	Lost
10	F	6	8	2	No	LTG	VPA	42	Y
11	F	10	6	1	No	LTG	No	54	Y
12	F	7	10	2	No	LTG	No	36	Y
13	M	9	20	1	No	LTG	No	56	Y (AEDs stopped)
14	M	7	7	1	No	LTG	No	58	Y (AEDs stopped)
15	F	5	5	1	No	LTG	VPA	58	Abandon
16	F	5	2	2	No	VPA	No	58	Y (AEDs stopped)
17	F	6	6	1	No	LTG	No	58	Y (AEDs stopped)
18	F	5	8	1	No	VPA	No	42	Y (AEDs stopped)
19	F	5	10	1	No	LTG	No	38	Y
20	F	4	4	2	No	VPA	LTG	43	Y
21	M	3	10	1	No	VPA	LTG	64	Y
22	F	5	10	2	No	VPA	LTG	60	Y
23	F	8	8	1	No	LTG	VPA/LEV	44	Y
24	F	10	7	1	No	LTG	No	65	Y
25	F	10	7	1	No	LEV stopped	LTG, VPA successively	64	Y

VPA valproic acid, *LTG* lamotrigine, *LEV* levetiracetam

was limited to 5 mm. The MEG signals were acquired at a sampling rate of 300 Hz, with noise cancellation of third-order gradients. During the MEG recordings, the subjects were asked to stay still and keep their eyes slightly closed. The subjects were also asked to avoid swallowing or teeth clenching. For each subject, at least six consecutive data files of a 2 min duration were collected. If no SWDs were observed in the MEG signals of the first three recorded files, the patients were instructed to hyperventilate to provoke seizures.

Magnetic Resonance Imaging (MRI) Scan

A total of 18 subjects accepted MRI scanning with a 3.0T scanner (Siemens, Germany), whereas a 1.5T scanner (Sigma, GE, USA) was used on seven subjects. The scan FOV was 240 mm; the FOV phase was 100%; the repetition time (TR) was 6600 ms; the echo time (TE) was 93 ms, and the slice thickness was 1.00 mm. MRI marks were placed in the locations of the three coils used in the MEG recordings to co-register the MRI and MEG data. All anatomical

landmarks digitized in the MEG study were rendered identifiable in the MRI.

Data Preprocessing

All MEG recordings without prolonged artifacts were retained. Only the SWDs of 3 Hz with a duration of longer than 10 s were analyzed in this study. Ictal onsets were determined by visual inspection. An ictal onset was defined by two criteria: (1) clearly distinguishable from the ongoing background rhythms and (2) unexplained by artifacts or physiologic changes. We calculated the dynamic source localization and functional connectivity (FC) during the ictal onset for 5 s in the two frequency bands from 23 patients (1–7 Hz and 8–30 Hz). Absence seizures from patients 24 and 25 started before the MEG recordings. Therefore, the initial portions of the ictal discharges were not recorded. The earliest 5 s recording was analyzed instead.

The determination of interictal data was completed in three steps: (1) finding a segment of interictal waveform that did not have SWDs ("clean interictal waveform"); (2) measuring the duration of the clean interictal waveform (> 30 s); and (3) checking if there were any 3 Hz SWDs before (pre-interval > 10 s) or after (post-interval > 10 s) the clean interictal waveform. If the duration of the clean interictal waveform was longer than 30 s and if both pre- and post-intervals were longer than 10 s, the "clean" interictal waveform was then selected as one segment of interictal data for the following data analysis. At least two segments of interictal data were analyzed for each subject.

Source Localization

We localized the significant neuromagnetic activities through accumulated source imaging (Xiang et al. 2014, 2015a), which was defined as the volumetric summation of the source activity over a period of time and was specifically developed and optimized to analyze activities in patients with CAE (Xiang et al. 2015a). Accumulated source imaging can be described by the following equation:

$$Asi(r,\ s) = \sum_{t=1}^{t=n} Q(r,\ t) \tag{1}$$

In Eq. (1), *Asi* represents the accumulated source strength at location *r; s* indicates the time slice; *t* indicates the time point of the MEG data; *n* indicates the total time points of the MEG data and *Q* indicates the source activity at source *r* and at time point *t*. We defined $s \geq 1$ and $s \leq n/2$. The source activity was computed by two-step beamforming (Xiang et al. 2015a). Specifically, the lead fields for each source (or voxel position) were computed to generate matrices with MEG data. The sensors selected for partial sensor coverage for each voxel with lead field (Xiang et al. 2015b), called voxel-based partial sensors, were used to minimize the effect of coherent sources in the source localization in the following beamformers. The covariance for voxel-based partial sensors was computed. Next, two sets of magnetic source images were computed using a vector beamformer (Xiang et al. 2015b). Then, the coherent source and the source orientation were estimated using the covariance matrix vector beamformer. Once the source orientation was determined, the final step was to generate the source activity (or virtual sensor waveform) with a scalar beamformer (Xiang et al. 2015b). The detailed mathematical algorithms and validations were described in recently published articles (Xiang et al. 2014, 2015a). In this paper, the whole brain was scanned at a 6-mm resolution (approximately 17,160 voxels/sources).

Functional Connectivity Analysis

Based on previous reports (Xiang et al. 2014, 2015a), FC was analyzed at the source level. To analyze FC at the source level, virtual sensor waveforms were computed for each source using the aforementioned algorithms. The source neural networks were estimated by analyzing the signal correlation of every pair of virtual sensors in the 5 s ictal time-windows. Specifically, the relationship of virtual sensor signals from the two-source pair was statistically analyzed by computing the correlation factor (or correlation coefficient). The correlation factors were defined by the following formulas:

$$R(X_a,\ X_b) = \frac{C(X_a,\ X_b)}{SX_{a,\ X_b}} \tag{2}$$

where $R\ (X_a, X_b)$ indicates the correlation of a source pair in two locations ("a" and "b"). The X_a and X_b indicate the signals in two sources, which were paired for computing connection. $C\ (X_a, X_b)$ represents the mean of the signals in the two sources. Sx_a and Sx_b indicate the standard deviation of the signals from the two sources. To avoid possible bias, we computed all possible connections for every two-source pair with source-level analyses. The distribution of the FC for each possible pair of all voxel-based virtual sensors was co-registered to individual participant MRIs (Xiang et al. 2014, 2015a). Magnetic source imaging-based neural networks were visualized in axial, coronal, and sagittal views to analyze the source connections. Blue and red were used to indicate inhibitory and excitatory connections, respectively. A threshold was used as a checkpoint to ensure the quality of the data. To determine the thresholding of connections, t values were computed for all source pairs.

$$\mathrm{Tp} = \mathrm{R}\sqrt{\frac{K-2}{1-R^2}} \tag{3}$$

In Eq. (3), Tp is the *t* value of a correlation; *R* indicates the correlation of a source pair; and *K* indicates the number of data points for the connection. In the present study, we used the Tp value that had a corresponding p value < 0.01 as the threshold to obtain the FC networks.

Statistical Analysis

An independent samples t test was used to analyze onset age and duration discharges between patients with an F–T–P/O network and patients with F–T networks or other networks at 1–7 Hz, as well as onset age and frequency between AED responders and AED non-responders. Levene's test for equality of variances was used. A chi-squared test (Fisher's exact test) was used to compare gender between patients with F–T–P/O networks and patients with F–T networks or other cortico–thalamic networks, as well as between AED responders and AED non-responders. The threshold of statistical significance for differences was set at $p < 0.05$ for each test. A Bonferroni correction was applied [for two frequency bands, $p < 0.025$ $(0.05/2 = 0.025)$]. All statistical analyses were performed with SPSS 19.0 for Windows (SPSS Inc., Chicago, IL, USA).

Results

Subjects

The gender ratio of the patients in the present study was 6:19 (male: female). The onset age was 7.32 ± 2.14 years. The seizure frequency was 8.8 ± 4.7 times/day. A total of 33 seizures with a duration of > 10 s were captured during the MEG recording. Eight seizures were provoked by hyperventilation. Thirty-one seizures were integrated, with an average duration of 20.5 ± 8.3 s. A total of 23 patients were followed-up successfully 36–66 months after the MEG was recorded. Fifteen patients were initially treated with LTG, and nine became seizure free with this treatment, whereas the other six continued to have seizures. One LTG non-responder gave up treatment due to VPA side effects. However, five LTG non-responders benefited from a VPA–LTG combination. A total of eight patients were initially treated with VPA, and five became seizure-free with this treatment, whereas the other three continued to have seizures. Moreover, three non-responders benefited from a VPA–LTG combination therapy. AEDs completely stopped in seven patients. Details of the data are shown in Table 1.

Source Location

Interictal sources at 1–7 Hz and 8–30 Hz were primarily localized in the occipital lobe (OL), precuneus (Pc) and thalamus. Ictal activation at 1–7 Hz was located in the ventral medial frontal cortex (VMFC) in nine seizures (abbreviated to $n = 9$), the post-dorsal medial frontal cortex (post-DMFC, including the medial primary motor cortex and the supplementary sensorimotor area, $n = 4$), the pre-dorsal medial frontal cortex (pre-DMFC, $n = 1$), the inferior parietal lobe (IPL, $n = 10$), the Pc ($n = 5$), and the OL ($n = 12$) (Table 2; Fig. 1). At 8–30 Hz, the source location was observed in the VMFC ($n = 6$), post-DMFC ($n = 10$), IPL ($n = 9$), Pc source location ($n = 5$), and OL ($n = 4$) (Table 2; Fig. 1). Source localization revealed that the sources were localized to the frontal cortex and the parietal cortex similarly for the 1–7 Hz and 8–30 Hz frequency bandwidths, whereas the occipital sources were primarily observed at the 1–7 Hz frequency bandwidth ($p = 0.006$). In our study, eight patients had two seizures with a duration of > 10 s. Although source imaging of seizures in a single patient may vary among seizures, there is consistency among different seizures in each patient (Fig. 2).

Cortico–Thalamic Functional Network

The inhibitory and excitatory connections constitute a cortico–thalamic network (Fig. 3). The inhibitory connections were primarily observed at 1–7 Hz ($p = 0.000$, Fig. 3c, d). The ictal 1–7 Hz recursive activities displayed the F–T–P/O networks ($n = 15$, Fig. 3a, b), F–T network ($n = 15$, Fig. 3e, f), fronto–thalamo–temporal network ($n = 1$), and parieto/occipito/temporal–thalamic network ($n = 2$, Table 2). At 1–7 Hz, the inhibitory connections were primarily observed in patients with F–T–P/O networks ($p = 0.005$). The ictal 8–30 Hz recursive activities were observed in the F–T–P/O networks ($n = 15$, Fig. 4a), F–T networks ($n = 9$, Fig. 4b), fronto–thalamo–temporal network ($n = 7$), and parieto/temporal–thalamic network ($n = 2$). At 1–7 Hz, patients with F–T–P/O networks were older than those with F–T networks or other cortico–thalamic networks ($p = 0.000$) (Tables 1, 2; Fig. 5a). The duration of seizures in patients with F–T–P/O networks at 1–7 Hz were longer than those with F–T or other cortico–thalamic networks ($p = 0.001$) (Table 2; Fig. 5b). No statistically significant differences were observed in gender between patients with F–T–P/O networks and patients with F–T networks or other cortico–thalamic networks at 1–7 Hz ($p = 0.645$).

Comparison Between Responders and Non-responders

The ictal post-DMFC source at 1–7 Hz or 8–30 Hz were observed in all (6/6) female LTG non-responders (Fig. 6). Interestingly, nine LTG responders showed no source locations in post-DMFC (Table 2). No statistically significant differences were observed in onset age ($p = 0.917$),

Table 2 Interictal and ictal source location and ictal cortico–thalamic network node

Patients	Interictal source location (1–7 Hz)	Interictal source location (8–30 Hz)	Ictal duration(s)	Ictal source location (1–7 Hz)	Ictal source location (8–30 Hz)	Ictal cortico–thalamic network node (1–7 Hz)	Ictal cortico–thalamic network node (8–30 Hz)
1	Bi Pc/OL	Bi Pc/OL	34.5	Bi post-DMFC; L IPL	VMFC	L pre-DMFC; R thalamus; L OL	Bi pre-DMFC; R thalamus; Bi Pc
2	L thalamus	L thalamus	22.2 (H) 17	Bi OL Bi OL; R OTJ	Bi post-DMFC; L CR L post-DMFC; L CR	VMFC; L thalamus; L IPL Bi D/VMFC; R thalamus	Bi pre-DMFC; R thalamus; R Pc L IPL; L thalamus
3	Bi OTJ	Bi Pc/OL	33.9	R Pc; R OL; R OTJ	R IPL; R OL; R Pc	L pre-DMFC; Bi thalamus; R IPL	L prefrontal lobe; Bi thalamus; L IPL
4	Bi thalamus	Bi thalamus	19.4 (H) 14.1	R OL; L IPL Bi OL	Bi post-DMFC Bi VMFC	Bi prefrontal lobe; Bi thalamus; R IPL R Bi D/VMFC; Bi thalamus; L IPL	R pre-DMFC; R thalamus; L IPL R pre-DMFC; R LFL; R thalamus; L Pc
5	L thalamus	Bi Pc/OL	23.6	Bi VMFC; R IPL	L thalamus	L VMFC; R LFL; Bi thalamus; R IPL	L prefrontal lobe; R LFL; R thalamus; R IPL
6	Bi Pc/OL	Bi Pc/OL	20.8 (H) 13.7	L IPL; Bi VMFC R OL; L IPL	L IPL R OL; R Pc	R prefrontal lobe; R thalamus; R IPL Bi pre-DMFC; L thalamus	R pre-DMFC; R thalamus; R IPL Bi pre-DMFC; R thalamus; L IPL
7	Bi Pc	Bi Pc/OL	35.5	Bi OL	R IPL	R pre-DMFC; Bi LFL; R thalamus; R IPL	L VMFC; R thalamus; R TL
8	Bi VMFC	Bi Pc/OL	18	Bi Pc; Bi OL	R post-DMFC; R LFL	L VMFC; L thalamus; R IPL	R LFL; Bi thalamus; R IPL; R TL
9	Bi Pc/OL	Bi Pc/OL	20	Bi post-DMFC; L IPL	Bi IPL	R LFL; L thalamus; Bi IPL	R prefrontal lobe; Bi thalamus; L Pc
10	Bi OL; L thalamus	Bi OL	36.6 (H) 25	L VMFC L VMFC	L post-DMFC L VMFC	R LFL; L thalamus; Bi Pc; Bi OL R LFL; R thalamus; R OL	Bi D/VMFC; Bi thalamus; L IPL Bi DMFC; Bi thalamus; L TL
11	Bi Pc	Bi Pc/OL	12	Bi Pc; Bi OL	R LFL	R LFL; Bi thalamus; L IPL	L LFL; R thalamus; R IPL
12	Bi Pc/OL	Bi Pc/OL	41 19.2	R IPL Bi Pc; Bi OL	L thalamus R Pc; R thalamus	L VMFC; Bi LFL; L thalamus R pre-DMFC; R thalamus; R IPL	R prefrontal lobe; Bi thalamus; L IPL R pre-DMFC; L thalamus
13	Bi VMFC	Bi thalamus	10	Bi VMFC	Bi VMFC	R pre-DMFC; R LFL; Bi thalamus	R LFL; R thalamus
14	Bi thalamus	L thalamus; Bi Pc/OL	10.5	L OL; L post TL	L post TL	Bi pre-DMFC; Bi thalamus	R LFL; Bi thalamus; L IPL
15	Bi OL	Bi OL	23.6 (H)	Bi VMFC	L post-DMFC	R VMFC; R thalamus; R post TL	R thalamus; R post TL

Table 2 (continued)

Patients	Interictal source location (1–7 Hz)	Interictal source location (8–30 Hz)	Ictal duration(s)	Ictal source location (1–7 Hz)	Ictal source location (8–30 Hz)	Ictal cortico–thalamic network node (1–7 Hz)	Ictal cortico–thalamic network node (8–30 Hz)
16	Bi VMFC; Bi Pc/OL	Bi VMFC; Bi Pc/OL	25.3 22.6	Bi IPL R IPL	Bi OL; Bi Pc L IPL	R pre-DMFC; R thalamus R pre-DMFC; R LFL; R thalamus	Bi pre-DMFC; R thalamus Bi VMFC; L thalamus
17	Bi Pc/OL	Bi Pc/OL	18	Bi VMFC	Bi Pc; Bi OL	Bi VMFC; L thalamus	Bi pre-DMFC; R thalamus
18	Bi VMFC	L thalamus	14.5	Bi OL; Bi Pc	L post-DMFC	Bi VMFC; L LFL; L thalamus	Bi VMFC; L thalamus
19	Bi Pc/OL	Bi Pc/OL	20.3 (H)	L post TL	L VMFC; L IPL	Bi VMFC; R thalamus	R pre-DMFC; Bi LFL; L IPL
20	Bi Pc/OL	Bi VMFC	16 13	R VMFC L post TL	L post-DMFC Bi VMFC; L IPL	R thalamus; Bi OL; Bi Pc Bi VMFC; L CR; Bi thalamus	Bi VMFC; Bi thalamus; L IPL R VMFC; Bi thalamus; Bi post TL
21	Bi Pc/OL	Bi Pc	10	Bi post-DMFC	R post-DMFC; R LFL	L pre-DMFC; R thalamus	Bi VMFC; R thalamus; R pre TL
22	Bi VMFC	Bi thalamus	10.3 17.7	L pre-DMFC L pre-DMFC; Bi IPL	L OTJ L OTJ	R pre-DMFC; L thalamus L LFL; R prefrontal lobe R thalamus	L thalamus; L IPL; L middle TL Bi VMFC; Bi thalamus; L pre TL
23	R IPL; L thalamus	L OL; L thalamus	10 (H)	L thalamus	L post-DMFC; L IPL	L thalamus; L IPL; L post TL	Bi VMFC; R thalamus
24	Bi Pc; Bi VMFC	Bi Pc/OL	18.3 (H)	Bi VMFC (internal 5s)	R IPL (internal 5s)	L prefrontal lobe; L thalamus; L Pc	Bi LFL; R thalamus
25	R OTJ; Bi thalamus	Bi OL	15.8 (H)	Bi post-DMFC (internal 5s)	L SPL (internal 5s)	R LFL; Bi thalamus; R IPL	R prefrontal lobe; R thalamus

Bi bilateral, *R* right, *L* left, *Post-DMFC* post-dorsal medial frontal cortex (including medial primary motor cortex and supplementary sensorimotor area), *VMFC* ventral medial frontal cortex, *Pc* precuneus, *OL* occipital lobe, *CR* central regions, *IPL* inferior parietal lobe, *OTJ* occipito–temporal junction, *LFL* lateral frontal lobe, *TL* temporal lobe, *SPL* superior parietal lobe, *H* hyperventilation

seizure frequency ($p = 0.294$), or cortico–thalamic network ($p = 0.545$) between LTG responders and LTG non-responders (Tables 1, 2). VPA responders were older than VPA non-responders ($p = 0.026$). In addition, the F–T–P/O networks were not observed in all VPA non-responders (Tables 1, 2). No statistically significant differences were observed in seizure frequency ($p = 0.597$) or gender ($p = 0.714$) between VPA responder and VPA non-responders (Tables 1, 2).

Discussion

In the current study, frequency-dependent neuromagnetic activities and cortico–thalamic interactions were investigated for a five-second window during the ictal period of absence seizure with MEG. To the best of our knowledge, this study is the first to study the associations between AED efficacy and the source localization and cortico–thalamic network in patients with CAE.

Our study demonstrated significant frontal source localization at 1–7 Hz and 8–30 Hz ($n = 25$, Table 2; Fig. 1). The frontal cortex has been reported to initiate and propagate absence seizures in previous scalp EEG, EEG–fMRI and MEG studies (Amor et al. 2009; Bai et al. 2010; Gupta et al. 2011; Holmes et al. 2004; Miao et al. 2014a, b; Szaflarski et al. 2010; Tang et al. 2015; Tenney et al. 2013, 2014; Westmijse et al. 2009), particularly in the medial frontal cortices (Bai et al. 2010; Miao et al. 2014a, b; Tang et al. 2015). In addition, negative blood oxygen level dependent (BOLD) changes in parietal source localization have been reported in previous EEG–fMRI studies of absence seizures (Bai et al. 2010; Carney et al. 2010; Masterton et al. 2013; Moeller et al. 2008; Vaudano et al. 2009). Vaudano et al. (2009) reported that Pc has a permissive function in absence seizures and in gating

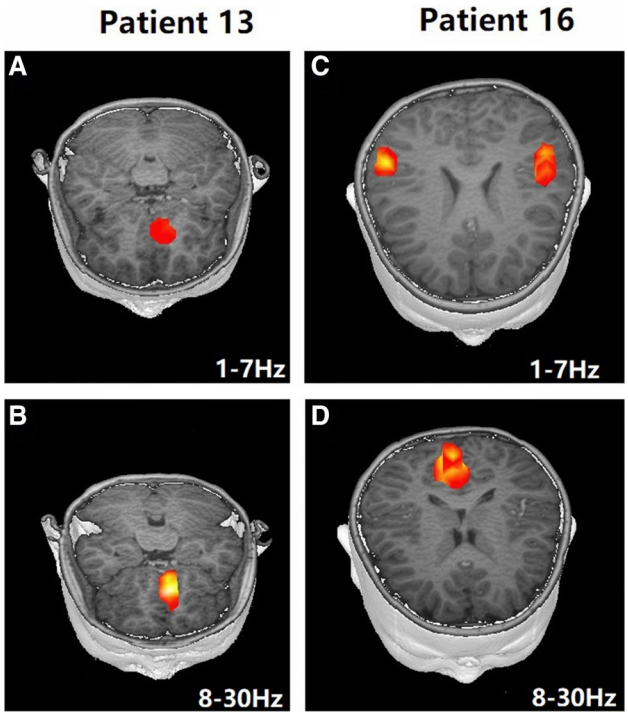

Fig. 1 VFMC source location (**a, b**), bilateral IPL (**c**), bilateral OL, and Pc (**d**) source location at 1–7 Hz and 8–30 Hz. *VMFC* ventral medial frontal cortex, *IPL* inferior parietal lobe, *Pc* precuneus, *OL* occipital lobe

SWDs in the epileptic network. When the spatial and temporal profiles of connectivity networks and sources in generalized SWDs were investigated in human absence epilepsy using MEG (Gupta et al. 2011), a low-frequency occipital source preceded a frontal cortical source prior to the first generalized spikes. In this study, we also revealed parietal source at the 1–7 Hz and 8–30 Hz in 22 seizures (Table 2; Fig. 1). Furthermore, the occipital sources were primarily observed at the 1–7 Hz frequency bandwidth in our study ($p = 0.006$). For generalized epileptic seizures, the ictal sources are not consistent from one seizure to another (Berg et al. 2010). Kokkinos et al. (2017) showed that for different consecutive seizures in one patient, the spatiotemporal distribution of the generalized ictal spikes remained fairly systematic. Although source imaging of seizures in a single patient may vary among seizures in our study, there is also consistency among different seizures in each patient (Fig. 2). The source localizations do not point to the abnormal brain tissues, but instead these localizations point to the areas engaged in dynamic networks in which the SWDs initiate and propagate. Single focus may not be the best way to understand the pathophysiology underlying seizure activity, and the analyses of networks or distributed processing in epilepsy should be prioritized (van Mierlo et al. 2014).

The cortico–thalamic circuit may be responsible for the 3 Hz SWDs (Luttjohann and van Luijtelaar 2015), and various cortical sources can be engaged in this network as long as the network is complete (Amor et al. 2009; Bai et al. 2010; Carney et al. 2010; Gupta et al. 2011; Holmes et al. 2004; Masterton et al. 2013; Miao et al. 2014a; Tang et al. 2015; Tenney et al. 2013, 2014; Vaudano et al. 2009; Westmijse et al. 2009; Szaflarski et al. 2010). In this study, the inhibitory and excitatory connections constituted a cortico–thalamic network. The fronto–thalamic connections observed in all patients played key roles in prolonging absence seizures (Table 2; Figs. 3, 4), which are thought to be the critical components of the rhythmic nature of SWDs during absence seizures (Bai et al. 2010; Miao et al. 2014a; Szaflarski et al. 2010; Tang et al. 2015; Tenney et al. 2013, 2014). The enhanced cortico–thalamic connectivity indicates that the cortex drove the thalamus early in the seizures (Wu et al. 2017). This finding is consistent with a simultaneous EEG–fMRI study that showed early fMRI increases in the orbital/medial frontal and medial/lateral parietal cortex > 5 s before seizure onset, while the thalamus showed delayed increases after seizure onset followed by small decreases (Bai et al. 2010). Spatiotemporal patterns of ictal spikes in the previous video-EEG study were identified to be of anteroposterior propagation and postero-anterior propagation and were confined to the frontal/prefrontal regions (Kokkinos et al. 2017). In accordance with the previous study (Kokkinos et al. 2017), our previous MEG study also showed ictal activity in the anterior (frontal cortices) and posterior cortices (parietal/occipital cortices) formed the main propagative pattern. The recursive propagations were through the middle of the brain (cortico–cortical pathways) or thalamus (cortico–thalamus–cortical pathways). This propagation was the main propagative pattern during the entirety of the absence seizures. In addition, the frontal sources propagated to the contralateral hemisphere also through cortico–cortical pathways (Miao et al. 2014a). The network between the thalamus and cortex was the focus of this study.

At 1–7 Hz, the cortico–thalamic–cortical network was associated with age (Tables 1, 2). The patients with an F–T–P/O network at 1–7 Hz were older than those with an F–T or other cortico–thalamic networks at 1–7 Hz (Fig. 5a). The maturation of the brain is associated with developmental change in spontaneous brain activities in a wide frequency range. The older children had a significantly stronger posterior cortical network connection, whereas the younger children had a significantly stronger anterior cortical network connection (Xiang et al. 2009). The network between the anterior and posterior cortices, including the default network, is strengthened during brain maturation. This finding is consistent with a recent fMRI report (Fair et al. 2008; Laufs et al. 2003; Xiang et al. 2009). The duration discharges in patients with an F–T–P/O network were longer than those

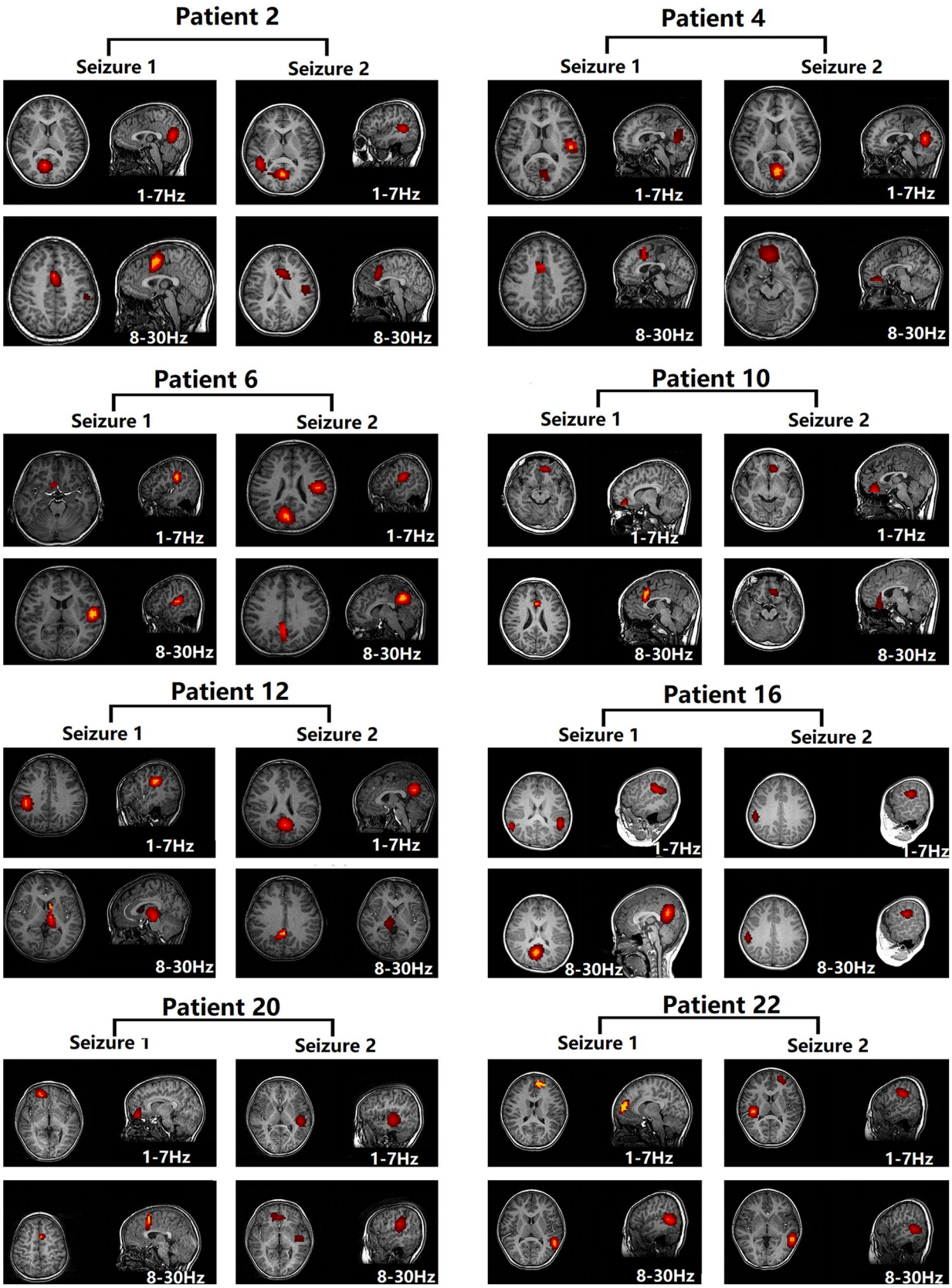

Fig. 2 Eight patients had two seizures with a duration of > 10 s. Source localization for different seizures. Although source imaging of seizures in a single patient may vary among seizures, there is consistency among different seizures in each patient

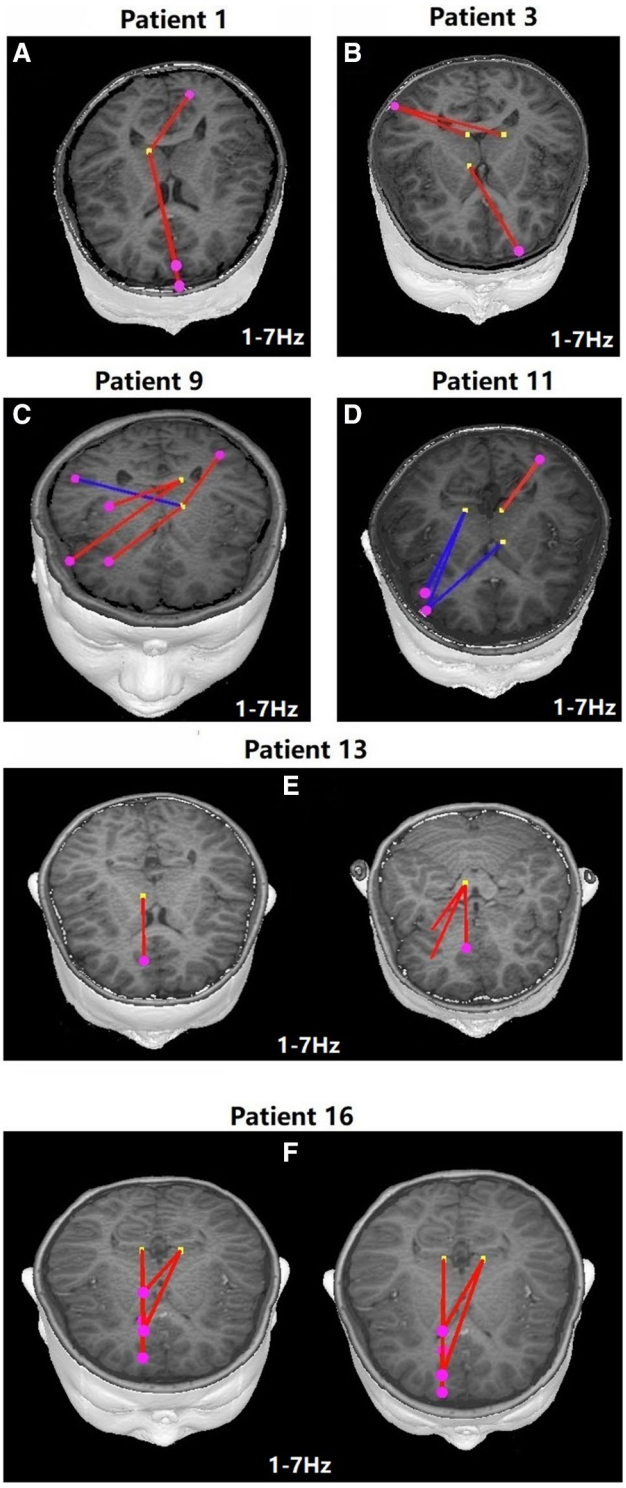

Fig. 3 The fronto–cortico–occipital functional connectivity (FC) (**a**) fronto–cortico–parietal FC (**b–d**), and fronto–thalamic FC (**e, f**) at 1–7 Hz. Patients 1, 3, 9 and 11 were older than patients 13 and 16. Yellow dot: thalamus; pink dot: the cortex. Blue: inhibitory connections; red: excitatory connections

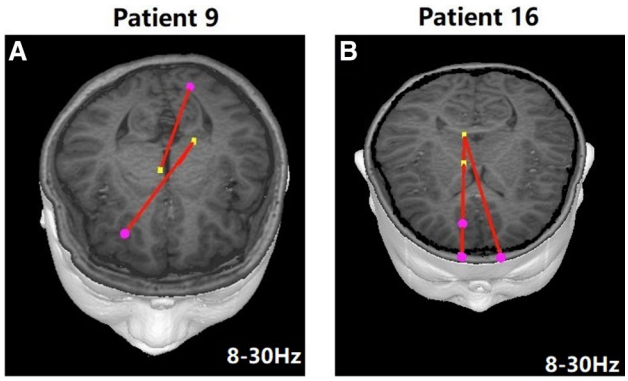

Fig. 4 The fronto–cortico–parietal functional connectivity (FC) (**a**) fronto–thalamic FC (**b**) at 8–30 Hz. Yellow dot: thalamus; pink dot: the cortex. Red: excitatory connections

with an F–T or other cortico–thalamic network at 1–7 Hz ($P < 0.05$, Fig. 5b), suggesting that the F–T–P/O network at 1–7 Hz plays an important role in duration discharges. The inhibitory connections were primarily observed in patients with an F–T–P/O network at 1–7 Hz, which might have effect of preventing excessive epileptic discharges (Fig. 3c, d). SWDs are generated within the cortico–thalamo–cortical system and that the integrity of this network is a prerequisite for the occurrence of "fully blown," bilateral, symmetrical SWDs (Bai et al. 2010; Wu et al. 2017; Luttjohann and van Luijtelaar 2015; Szaflarski et al. 2010; Tenney et al. 2013, 2014). The cortico–thalamo–cortical network consists of anterior and posterior cortices, which might contribute to the maintenance of discharges.

We searched for imaging markers indicating AED treatment responsiveness in this study. Post-DMFC source localizations were observed in all LTG non-responders, but not in all LTG responders (Table 2; Fig. 6). In a study of genetic absence epilepsy rats, increased basal γ-aminobutyric acid (GABA) levels and decreased basal glutamate level in the primary motor cortex were noted, denoting the generation and the initiation of absence seizures (Terzioğlu et al. 2006). Systemic injection of ETX reduced the GABA levels in the primary motor cortex (Terzioğlu et al. 2006). Post-DMFC source localizations suggest that children with CAE might experience initial LTG monotherapy failure. One LTG non-responders gave up treatment due to VPA side effects, but benefited from a VPA–LTG combination treatment (Tables 1, 2). A total of three out of five patients with post-DMFC source localizations and initial VPA monotherapy became seizure-free. Previous retrospective studies in CAE have hinted that VPA could be more effective than LTG in this population (Glauser et al. 2010, 2013). Patients with post-DMFC source localizations might either be indirectly treated with VPA monotherapy or an accepted VPA–LTG combination. A total of three VPA non-responders also

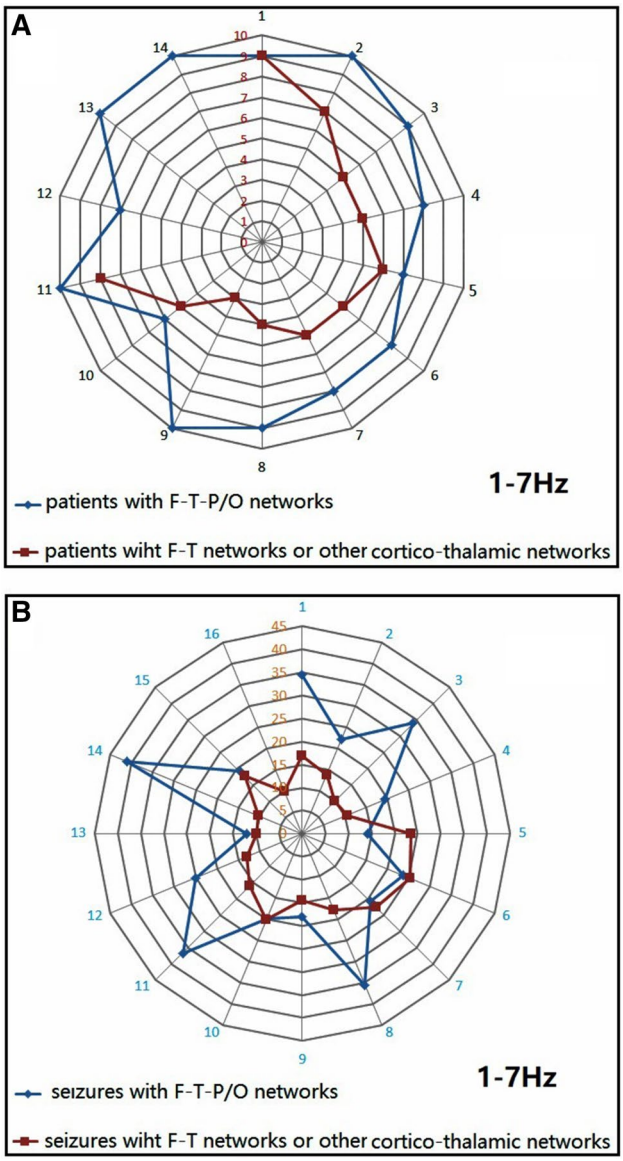

Fig. 5 Radar diagram: **a** Patients with F–T–P/O networks were older than those with F–T networks or other cortico–thalamic networks at 1–7 Hz ($p=0.000$). Black numbers: number of patients; red numbers: onset age. **b** The duration of seizures in patients with F–T–P/O networks was longer than those with F–T or other cortico–thalamic networks at 1–7 Hz ($p=0.001$). Light blue numbers: number of seizures; brown numbers: duration of seizures

achieved seizure freedom with VPA–LTG combination therapy. Some evidence suggests that LTG, in combination with VPA, may work synergistically to provide superior seizure control than the use of each drug independently. Early case studies report dramatic reductions in seizure frequency when LTG is added to VPA in patients with absence seizures (Ferrie et al. 1995; Panayiotopoulos et al. 1993). Although the efficacy of the VPA–LTG combination can be superior to either drug given separately, the precise mechanism underlying the pharmacodynamic interactions remains to be clarified. LTG is considered to suppress seizures by inhibiting the release of the excitatory amino acid glutamate through sodium channel blockade (Fitton and Goa 1995; Leach et al. 1986), whereas VPA may block sodium channels, increase presynaptic GABA content, and release and enhance postsynaptic activation at GABA-receptor sites (MacDonald and Bergey 1979). These mechanisms may explain the complementary effects. Other modes of action have been described for VPA (Davis et al. 1994) and LTG (Stefani et al. 1997), and their precise interaction at the molecular level remains unclear.

We also investigated whether there were associations between the cortico–thalamic network and AED efficacy. No statistically significant differences were observed in the cortico–thalamic network ($p=0.545$) between LTG responders and LTG non-responders. The mechanism of LTG is to inhibit the release of the excitatory amino acid glutamate through sodium channel blockade (Fitton and Goa 1995; Leach et al. 1986). Generalized epileptic seizures are conceptualized as originating at some point at which the excitatory amino acid increases significantly (Berg et al. 2010). LTG efficacy is associated with focal regions involved with increasing excitatory amino acid. In this study, post-DMFC source localizations suggest that children with CAE might experience initial LTG monotherapy failure. VPA may block sodium channels and increase presynaptic and postsynaptic GABA effect in the whole brain, not focal regions (MacDonald and Bergey 1979). VPA efficacy might be associated with the sophistication of the brain network. The connection between anterior and posterior cortices is strengthened during brain maturation (Fair et al. 2008). In this study, VPA responders were older than VPA non-responders (Tables 1, 2). The cortico-thalamic network was associated with age. At 1–7 Hz, the older children showed an F–T–P/O network, but younger children showed an F–T network. Young onset age is a refractory epilepsy risk factor (Wirrell et al. 2012).

Several limitations of the present study should be considered. Because of the relatively low spatial resolution of MEG, localizing each thalamic nucleus in human is difficult, and researchers always regarded the thalamus in its entirety (Miao et al. 2014a; Tenney et al. 2013), including in many studies using fMRI (Bai et al. 2010; Carney et al. 2010; Liao et al. 2014). The localization of deep sources is debatable in the current MEG field. MEG might have low spatial resolution of this localizer within deep structures. Increasing evidence has demonstrated that MEG can detect neuromagnetic signals from deep structures, and the spatial resolution is sufficient in many studies (Attal and Schwartz 2013; Balderston et al. 2013; Papadelis et al. 2009; Quraan et al. 2011). Another limitation of this study is the low number of subjects and the number of ictal seizures analyzed. Given that approximately 40% of patients with CAE will become LTG treatment non-responders, a larger sample of

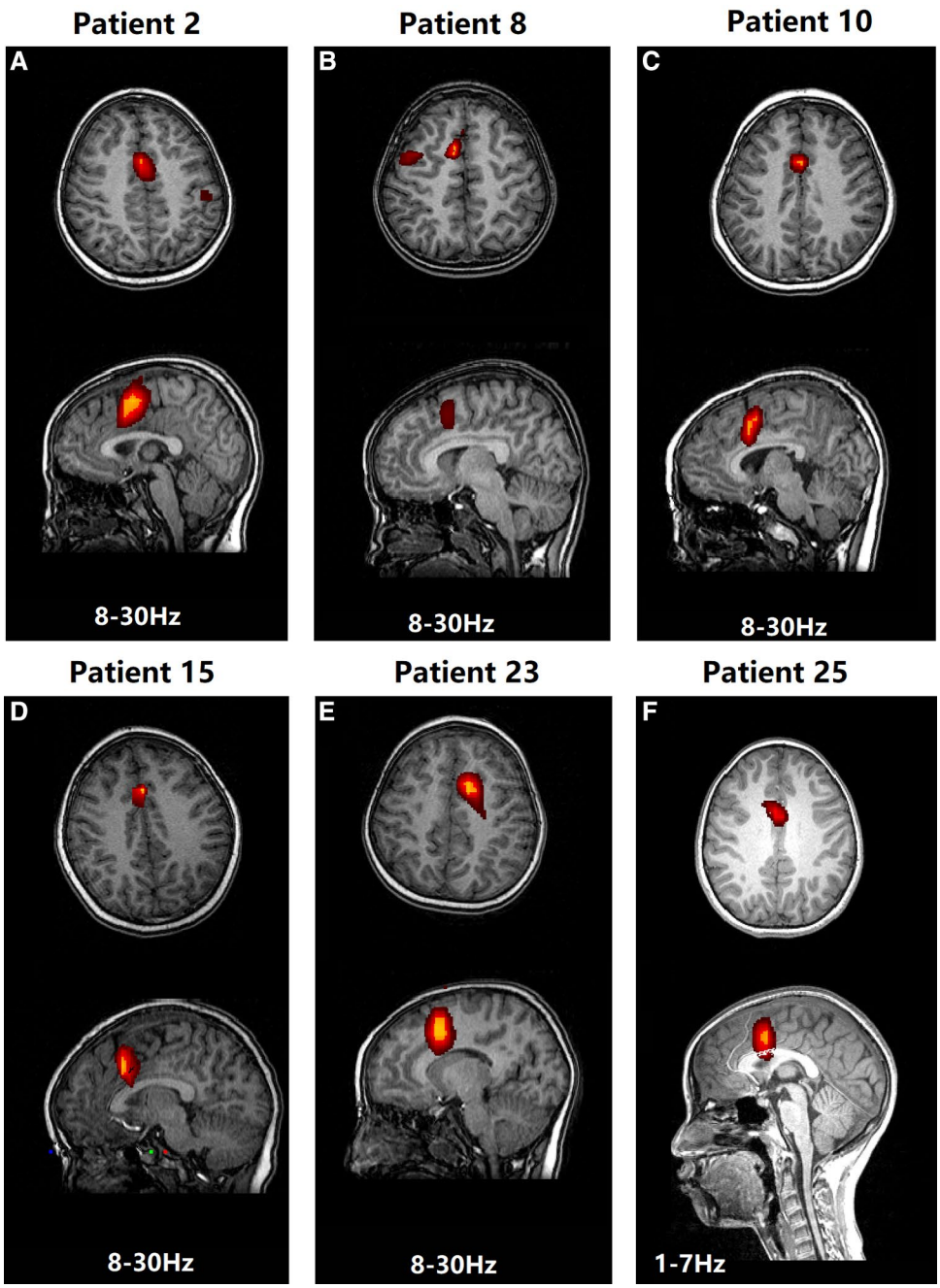

Fig. 6 Post-DMFC source locations in six LTG non-reponders. *LTG* lamotrigine, *Post-DMFC* post-dorsal medial frontal cortex (including medial primary motor cortex and supplementary sensorimotor area)

newly diagnosed patients with CAE would be important for the validation of our findings. In addition, the treatment response was susceptible to the observation of the guardian, though the guardians were repeatedly reminded to observe the absence seizures.

In this study, source locations provided useful information for CAE treatment. The VMFC, DMFC, IPL, Pc and OL served as important component in absence seizures. Children with CAE with post-DMFC source localizations might experience initial LTG monotherapy failure. The cortico–thalamo–cortical network is associated with age. The cortico–thalamo–cortical network consisting of anterior and posterior cortices might contribute to the maintenance of discharges.

Acknowledgements This work was supported by the National Natural Science Foundation of China (Grant Nos. 81501126 and 81471324), Young Medical Key Talents Foundation of Jiangsu Province (Grant No. QNRC2016053), Training Project for Young Talents of Nanjing Brain Hospital, Key Project of Medical Science and Technology Development Foundation (Grant No. ZKX11002), Fourth Phase of Jiangsu "Project 333" Scientific Research Funding Schemes, 2013, Health Department of Jiangsu Province (Grant No. H201443), the Nanjing

Medical University General Program (Grant Nos. 2014NJMU050 and 2017NJMU143).

Compliance with Ethical Standards

Conflict of interest None of the authors has any conflict of interest to disclose.

Ethical Approval We confirm that we have read the Journal's position on issues involved in ethical publication and affirm that this report is consistent with those guidelines.

References

Amor F, Baillet S, Navarro V, Adam C, Martinerie J, Le Van Quyen M (2009) Cortical local and long-range synchronization interplay in human absence seizure initiation. NeuroImage 45:950–962. https://doi.org/10.1016/j.neuroimage.2008.12.011

Attal Y, Schwartz D (2013) Assessment of subcortical source localization using deep brain activity imaging model with minimum norm operators: a MEG study. PLoS ONE. https://doi.org/10.1371/journal.pone.0059856

Bai X, Vestal M, Berman R, Negishi M, Spann M, Vega C, Desalvo M, Novotny EJ, Constable RT, Blumenfeld H (2010) Dynamic time course of typical childhood absence seizures: EEG, behavior, and functional magnetic resonance imaging. J Neurosci 30:5884–5893. https://doi.org/10.1523/JNEUROSCI.5101-09.2010

Balderston NL, Schultz DH, Baillet S, Helmstetter FJ (2013) How to detect amygdala activity with magnetoencephalography using source imaging. J Vis Exp. https://doi.org/10.3791/50212

Berg AT, Shinnar S, Levy SR, Testa FM, Smith-Rapaport S, Beckerman B (2000) How well can epilepsy syndromes be identified at diagnosis? A reassessment 2 years after initial diagnosis. Epilepsia 41:1269–1275

Berg AT, Berkovic SF, Brodie MJ (2010) Revised terminology and concepts for organization of seizures and epilepsies: report of the ILAE Commission on Classification and Terminology, 2005–2009. Epilepsia 51:676–685. https://doi.org/10.1111/j.1528-1167.2010.02522.x

Bouma PA, Westendorp RG, van Dijk JG, Peters AC, Brouwer OF (1996) The outcome of absence epilepsy: a meta-analysis. Neurology 47:802–808

Carney PW, Masterton RAJ, Harvey AS, Scheffer IE, Berkovic SF, Jackson GD (2010) The core network in absence epilepsy. Neurology 75:904–911. https://doi.org/10.1212/WNL.0b013e3181f11c06

Commission on Classification and Terminology of the International League Against Epilepsy (1989) Proposal for revised classification of epilepsies and epileptic syndromes. Epilepsia 30:389–399

Davis R, Peters DH, McTavish D (1994) Valproic acid: a reappraisal of its pharmacological properties and clinical efficacy in epilepsy. Drugs 2:332–372

Fair DA, Cohen AL, Dosenbach NU, Church JA, Miezin FM, Barch DM, Raichle ME, Petersen SE, Schlaggar BL (2008) The maturing architecture of the brain's default network. Proc Natl Acad Sci 105:4028–4032. https://doi.org/10.1073/pnas.0800376105

Ferrie CD, Robinson RO, Knott C, Panayiotopoulos CP (1995) Lamotrigine as an add-on drug in typical absence seizures. Acta Neurol Scand 91:200–202

Fitton A, Goa KL (1995) Lamotrigine: an update of its pharmacology and therapeutic use in epilepsy. Drugs 50:691–713

Gadad V, Sinha S, Mariyappa N, Velmurugan J, Chaitanya G, Sain J, Thennarasu K, Satishchandra P (2018) Source analysis of epileptiform discharges in absence epilepsy using Magnetoencephalography (MEG). Epilepsy Res 140:46–52. https://doi.org/10.1016/j.eplepsyres.2017.12.003

Glauser TA1, Cnaan A, Shinnar S, Hirtz DG, Dlugos D, Masur D, Clark PO, Capparelli EV, Adamson PC, Childhood Absence Epilepsy Study Group (2010) Ethosuximide, valproic acid, and lamotrigine in childhood absence epilepsy. N Engl J Med 362:790–799. https://doi.org/10.1056/NEJMoa0902014

Glauser TA1, Cnaan A, Shinnar S, Hirtz DG, Dlugos D, Masur D, Clark PO, Capparelli EV, Adamson PC, Childhood Absence Epilepsy Study Group (2013) Ethosuximide, valproic acid, and lamotrigine in childhood absence epilepsy: initial monotherapy outcomes at 12 months. Epilepsia 54:141–155. https://doi.org/10.1111/epi.12028

Gupta D, Ossenblok P, van Luijtelaar G (2011) Space-time network connectivity and cortical activations preceding spike wave discharges in human absence epilepsy: a MEG study. Med Biol Eng Comput 49:555–565. https://doi.org/10.1007/s11517-011-0778-3

Holmes MD, Brown M, Tucker DM (2004) Are generalized seizures truly generalized? Evidence of localized mesial frontaland frontopolar discharges in absence. Epilepsia 45:1568–1579

Jallon P, Loiseau P, Loiseau J (2001) Newly diagnosed unprovoked epileptic seizures: presentation at diagnosis in CAROLE study. Epilepsia 42:464–475

Kokkinos V, Koupparis AM, Koutroumanidis M, Kostopoulos GK (2017) Spatiotemporal propagation patterns of generalized ictal spikes in childhood absence epilepsy. Clin Neurophysiol 128:1553–1562. https://doi.org/10.1016/j.clinph.2017.05.021

Laufs H, Krakow K, Sterzer P, Eger E, Beyerle A, Salek-Haddadi A, Kleinschmidt A (2003) Electroencephalographic signatures of attentional and cognitive default modes in spontaneous brain activity fluctuations at rest. Proc Natl Acad Sci 100:11053–11058. https://doi.org/10.1073/pnas.1831638100

Leach MJ, Marden CM, Miller AA (1986) Pharmacological studies on lamotngine, a novel potential antiepileptic drug. 11. Neurochemical studies on the mechanism of action. Epilepsia 27:490–497

Liao W, Zhang Z, Mantini D, Xu Q, Ji GJ, Zhang H, Wang J, Wang Z, Chen G, Tian L, Jiao Q, Zang YF, Lu G (2014) Dynamical intrinsic functional architecture of the brain during absence seizures. Brain Struct Funct 219:2001–2015. https://doi.org/10.1007/s00429-013-0619-2

Loiseau P, Duché B, Pédespan JM (1995) Absence epilepsies. Epilepsia 36:1182–1186

Luttjohann A, van Luijtelaar G (2015) Dynamics of networks during absence seizure's on-and offset in rodents and man. Front Physiol. https://doi.org/10.3389/fphys.2015.00016

MacDonald RL, Bergey GK (1979) Valproic acid augments GABA mediated post-synaptic inhibition in cultured mammalian neurones. Brain Res 170:558–562

Masterton RA, Carney PW, Abbott DF, Jackson GD (2013) Absence epilepsy subnetworks revealed by event-related independent components analysis of functional magnetic resonance imaging. Epilepsia 54:801–808. https://doi.org/10.1111/epi.12163

Meeren HK, Pijn JP, Van Luijtelaar EL (2002) Cortical focus drives widespread corticothalamic networks during spontaneous absence seizures in rats. J Neurosci 22:1480–1495

Meeren H, van Luijtelaar G, Lopes da Silva F, Coenen A (2005) Evolving concepts on the pathophysiology of absence seizures. Arch Neurol 62:371–376. https://doi.org/10.1001/archneur.62.3.371

Miao A, Tang L, Xiang J, Guan Q, Ge H, Liu H, Wu T, Chen Q, Yang L, Lu X, Hu Z, Wang X (2014a) Dynamic magnetic source imaging of absence seizure initialization and propagation: a magnetoencephalography study. Epilepsy Res 108:468–480. https://doi.org/10.1016/j.eplepsyres.2014.01.006

Miao A, Xiang J, Tang L, Ge H, Liu H, Wu T, Chen Q, Hu Z, Lu X, Wang X (2014b) Using ictal high-frequency oscillations (80-500Hz) to localize seizure onset zones in childhood absence epilepsy: a MEG study. Neurosci Lett 566:21–26. https://doi.org/10.1016/j.neulet.2014.02.038

Moeller F, Siebner HR, Wolff S, Muhle H, Granert O, Jansen O, Stephani U, Siniatchkin M (2008) Simultaneous EEG-fMRI in drug-naive children with newly diagnosed absence epilepsy. Epilepsia 49:1510–1519. https://doi.org/10.1111/j.1528-1167.2008.01626.x

Panayiotopoulos CP, Ferrie CD, Knott C, Robinson RO (1993) Interaction of lamotrigine with sodium valproate. Lancet 341:445

Papadelis C, Poghosyan V, Fenwick PB, Ioannides AA (2009) MEG's ability to localise accurately weak transient neural sources. Clin Neurophysiol 120:1958–1970. https://doi.org/10.1016/j.clinph.2009.08.018

Pavone P, Bianchini R, Trifiletti RR, Incorpora G, Pavone A, Parano E (2001) Neuropsychological assessment in children with absence epilepsy. Neurology 56:1047–1051

Quraan MA, Moses SN, Hung Y, Mills T, Taylor MJ (2011) Detection and localization of hippocampal activity using beamformers with MEG: a detailed investigation using simulations and empirical data. Hum Brain Mapp 32:812–827. https://doi.org/10.1002/hbm.21068

Stefani A, Spadoni F, Bemardi G (1997) Voltage-activated calcium channels: targets of antiepileptic drug therapy? Epilepsia 38:959–965

Szaflarski JP, DiFrancesco M, Hirschauer T, Banks C, Privitera MD, Gotman J, Holland SK (2010) Cortical and subcortical contributions to absence seizure onset examined with EEG/fMRI. Epilepsy Behav 18:404–413. https://doi.org/10.1016/j.yebeh.2010.05.009

Tang L, Xiang J, Huang S, Miao A, Ge H, Liu H, Wu D, Guan Q, Wu T, Chen Q, Yang L, Lu X, Hu Z, Wang X (2015) Neuromagnetic high-frequency oscillations correlate with seizure severity in absence epilepsy. Clin Neurophysiol 127:1120–1129. https://doi.org/10.1016/j.clinph.2015.08.016

Tenney JR, Fujiwara H, Horn PS, Jacobson SE, Glauser TA, Rose DF (2013) Focal corticothalamic sources during generalized absence seizures: a MEG study. Epilepsy Res 106:113–122. https://doi.org/10.1016/j.eplepsyres.2013.05.006

Tenney JR, Fujiwara H, Horn PS, Vannest J, Xiang J, Glauser TA, Rose DF (2014) Low- and high-frequency oscillations reveal distinct absence seizure networks. Ann Neurol 76:558–567. https://doi.org/10.1002/ana.24231

Terzioğlu B, Aypak C, Onat FY, Küçükibrahimoğlu E, Ozkaynakçi AE, Gören MZ (2006) The effects of ethosuximide on amino acids in genetic absence epilepsy rat model. J Pharmacol Sci 100:227–233

van Luijtelaar G, Sitnikova E (2006) Global and focal aspects of absence epilepsy: the contribution of genetic models. Neurosci Biobehav Rev 30:983–1003. https://doi.org/10.1016/j.neubiorev.2006.03.002

van Mierlo P, Papadopoulou M, Carrette E, Boon P, Vandenberghe S, Vonck K, Marinazzo D (2014) Functional brain connectivity from EEG in epilepsy: seizure prediction and epileptogenic focus localization. Prog Neurobiol 121:19–35. https://doi.org/10.1016/j.pneurobio.2014.06.004

Vaudano AE, Laufs H, Kiebel SJ, Carmichael DW, Hamandi K, Guye M, Thornton R, Rodionov R, Friston KJ, Duncan JS, Lemieux L (2009) Causal hierarchy within the thalamo-cortical network in spike and wave discharges. PLoS ONE. https://doi.org/10.1371/journal.pone.0006475

Westmijse I, Ossenblok P, Gunning B, van Luijtelaar G (2009) Onset and propagation of spike and slow wave discharges in human absence epilepsy: a MEG study. Epilepsia 50:2538–2548. https://doi.org/10.1111/j.1528-1167.2009.02162.x

Wheless JW, Clarke DF, Carpenter D (2005) Treatment of pediatric epilepsy: expert opinion. J Child Neurol 20(Suppl 1):S1–S56

Wirrell EC, Camfield CS, Camfield PR, Dooley JM, Gordon KE, Smith B (1997) Long-term psychosocial outcome in typical absence epilepsy: sometimes a wolf in sheeps' clothing. Arch Pediatr Adolesc Med 151:152–158

Wirrell E, Wong-Kisiel L, Mandrekar J, Nickels K (2012) Predictors and course of medically intractable epilepsy in young children presenting before 36 months of age: a retrospective, population-based study. Epilepsia 53:1563–1569. https://doi.org/10.1111/j.1528-1167.2012.03562.x

Wu C, Xiang J, Sun J, Huang S, Tang L, Miao A, Zhou Y, Chen Q, Hu Z, Wang X (2017) Quantify neuromagnetic network changes from pre-ictal to ictal activities in absence seizures. Neuroscience 357:134–144. https://doi.org/10.1016/j.neuroscience

Xiang J, Liu Y, Wang Y, Kotecha R, Kirtman EG, Chen Y, Huo X, Fujiwara H, Hemasilpin N, De Grauw T, Rose D (2009) Neuromagnetic correlates of developmental changes in endogenous high-frequency brain oscillations in children: a wavelet-based beamformer study. Brain Res 1274:28–39. https://doi.org/10.1016/j.brainres.2009.03.068

Xiang J, Luo Q, Kotecha R, Korman A, Zhang F, Luo H, Fujiwara H, Hemasilpin N, Rose DF (2014) Accumulated source imaging of brain activity with both low and high-frequency neuromagnetic signals. Front Neuroinform. https://doi.org/10.3389/fninf.2014.00057

Xiang J, Tenney JR, Korman AM, Leiken K, Rose DF, Harris E, Yuan W, Horn PS, Holland K, Loring DW, Glauser TA (2015a) Quantification of interictal neuromagnetic activity in absence epilepsy with accumulated source imaging. Brain Topogr 28:904–914. https://doi.org/10.1007/s10548-014-0411-5

Xiang J, Korman A, Samarasinghe KM, Wang X, Zhang F, Qiao H, Sun B, Wang F, Fan HH, Thompson EA (2015b) Volumetric imaging of brain activity with spatial-frequency decoding of neuromagnetic signals. J Neurosci Methods 239:114–128. https://doi.org/10.1016/j.jneumeth.2014.10.007